Pore Structural Complexities and Gas Storage Capacity of Indian Coals with Various Thermal Maturities

Hazra, Bodhisatwa; Wood, David A.; Panda, Mahima; Sethi, Chinmay; Vishal, Vikram; Chandra, Debanjan; Ostadhassan, Mehdi

DOI
10.1021/acs.energyfuels.5c00021

Publication date
2025

Document Version
Final published version

Published in
Energy and Fuels

Citation (APA)
Hazra, B., Wood, D. A., Panda, M., Sethi, C., Vishal, V., Chandra, D., & Ostadhassan, M. (2025). Pore Structural Complexities and Gas Storage Capacity of Indian Coals with Various Thermal Maturities. *Energy and Fuels*, *39*(12), 5818-5831. https://doi.org/10.1021/acs.energyfuels.5c00021

energy&fuels

Open Access

pubs.acs.org/EF Article

Pore Structural Complexities and Gas Storage Capacity of Indian Coals with Various Thermal Maturities

Bodhisatwa Hazra,* David A Wood, Mahima Panda, Chinmay Sethi, Vikram Vishal, Debanjan Chandra, and Mehdi Ostadhassan*

Cite This: *Energy Fuels* 2025, 39, 5818−5831 Read Online

ABSTRACT: Understanding pore structural complexities of coal is essential in coalbed methane (CBM) enhanced recovery and optimization of CO_2 sequestration strategies. Coal's micropores play a pivotal role in gas adsorption, while its mesopores and macropores facilitate gas migration and recovery. This study investigates the relationship between thermal maturity, maceral composition, and pore structural attributes in five coal samples with progressing thermal maturity from the Raniganj and Jharia Basins, India, using low-pressure nitrogen (N_2) and carbon dioxide (CO_2) adsorption techniques. A key focus is to derive fractal dimensions from CO_2 adsorption data, which effectively captures micropore complexity and heterogeneity, offering critical insights into the coal's gas storage potential. The results reveal that thermal maturity significantly impacts pore development, with postmature coals exhibiting greater micropore volumes and higher fractal dimensions, indicating higher complexity of the pore surface area and gas storage capacity. The analysis of the CO_2 adsorption data proved superior to the N_2 ones in characterizing micropores, which contribute significantly in estimating the maximum gas adsorption potential of coal. This study highlights strong correlations between fractal dimensions, maceral composition, and thermal maturity markers obtained from programmed pyrolysis. This work highlights that CO_2-derived fractal dimension analysis coupled with organic petrography and the Rock-Eval thermal maturity parameter can be an effective way to understand the surface heterogeneity of micropores in coals and its implications for gas storage.

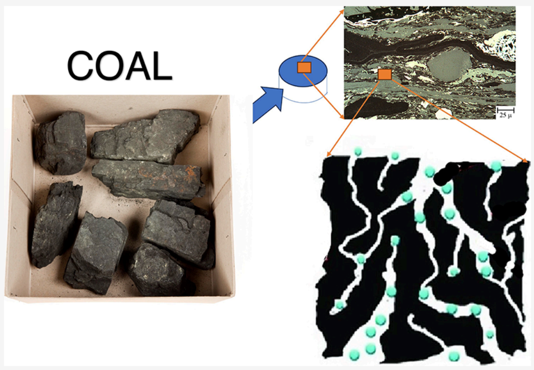

1. INTRODUCTION

Coal's pore structure plays a pivotal role in the storage capacity of coalbed methane (CBM) and its suitability for CO_2 sequestration.[1,2] In CBM extraction, an intricate pore network enhances methane adsorption in micropores, which offer extensive surface area for gas-molecule adsorption, while larger meso- and macropores facilitate gas migration pathways, supporting gas flow and recovery.[3−6] Similarly, in CO_2 sequestration, coal's complex pore system allows for efficient CO_2 adsorption within micropores and allows for gas diffusion in mesopores.[7,8] Therefore, a comprehensive understanding of coal formation's pore structure and pore size distribution is essential for optimizing CBM recovery, maximizing CO_2 storage potential, and identifying the feasibility of specific coal formations as carbon capture and storage (CCS) repositories.

Significant research has been conducted to classify pore structures of solids, tailored to different research objectives and levels of measurement precision.[9,10] The classification of pores by the International Union of Pure and Applied Chemistry[11] organizes pores into three categories based on their size: micropores are smaller than 2 nm, mesopores range from 2 to 50 nm, and macropores are larger than 50 nm. Coal's complex pore characteristics encompass a range of parameters, including pore size distribution (PSD), pore morphology, pore volume, specific surface area (SSA), and pore network structure.[12−14] In recent years, various experimental techniques have been employed to analyze coal's internal structure, such as scanning electron microscopy (SEM), mercury intrusion porosimetry (MIP), small-angle X-ray scattering (SAXS), and physisorption methods.[15−18] Among these, low-pressure nitrogen (N_2) and carbon dioxide (CO_2) gas adsorptions are commonly used to study the coal pore properties effectively. Since adsorption is a surface-related phenomenon, analyzing the surface characteristics of pores in the coal is essential to understanding gas storage mechanisms. As a gas injection-based method, adsorption aids in assessing pores of diverse shapes and sizes, accurately measuring

Received: January 3, 2025
Revised: March 3, 2025
Accepted: March 4, 2025
Published: March 13, 2025

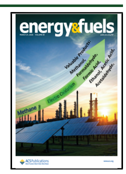

surface area, pore size distribution, and fractal dimensions from the adsorption isotherms.[16]

Fractal dimension analysis is a key aspect of understanding the pore structure of coal, which delineates the complexity, roughness, and heterogeneity of the pore surface.[19,20] In this regard, larger fractal dimensions infer more surface complexity, meaning the presence of more active sites for gas adsorption.[4] N_2 adsorption is a widely accepted technique for calculating the fractal dimension of coal and shale pore structures, where adsorption isotherms are used to derive this parameter through methods such as the Frenkel−Halsey−Hill (FHH) or the modified Frenkel−Halsey−Hill (MFHH) model.[4,21−23] However, extracting fractal dimensions using the MFHH method involves uncertainties and requires customized curve fitting techniques to the isotherm data.[24]

While N_2 adsorption is generally used to determine the fractal dimension of pores, it has certain limitations in delineating the complexity of the pore structures fully. Specifically, N_2 molecules, due to their relatively larger size, have restricted access to smaller micropores (<2 nm) within the coal matrix.[6,25,26] This limitation means that N_2 adsorption primarily provides fractal details representing mesopores and macropores, which eludes the understanding of the microporous network. Studies have shown that alternative adsorbates, such as CO_2, can access smaller micropores more effectively, yielding a more comprehensive view of pore size distribution and surface complexity, which is critical for assessing gas storage potential.[8,27,28] Since micropores are the primary contributors to gas adsorption due to their significantly larger specific surface area than mesopores,[29] a combination of N_2 adsorption for mesopores and low-pressure CO_2 adsorption for micropores is essential to accurately determine fractal dimensions and effectively characterize the entire pore structure within coal.

In recent years, some studies have determined fractal dimensions using the "micropore fractal model" obtained from CO_2 adsorption parameters.[29−31] Nie et al.[29] used low-pressure N_2 and CO_2 gas adsorption methods to analyze the pore distribution and fractal dimension features of coal samples at various metamorphic phases. They found a correlation between the gas flow patterns in coal seams and coal pore structures. They discovered that when metamorphism increased, pore formation improved and the fractal dimensions of micropores and mesopores shifted proportionally. Outburst coals (defined by moderate to high levels of metamorphism), which have higher pore volumes, specific surface areas, and more complex microstructures, exhibit significant heterogeneity in micropores compared to nonoutburst coals. Similarly, Shi et al.[31] calculated the CO_2-based fractal dimension and observed that intense tectonic deformation significantly alters shale pore structures, particularly micropores. Under strong compression, micropore volume and surface area increase as mesopores are compacted, with fractal analysis showing that micropore fractal dimensions (Df) decrease with increasing burial depth.

Considering the importance of coal pore structure evolution as it undergoes metamorphism, as well as the advantages that this rock type can provide us with storage of CO_2 and production of methane, this study comprehensively analyzes the complexities of coal sample pore structures with varying thermal maturation backgrounds using low-pressure CO_2 and N_2 gas adsorption techniques, with a particular emphasis on CO_2-based fractal dimension analysis. Building on previous investigations into the thermal properties of coals from the Raniganj and Jharia Basins,[32] five representative coal samples with distinct thermal histories and petrographic compositions were selected to evaluate the effects of thermal maturity on pore structural properties in particular. CO_2 adsorption-derived fractal dimensions for micropores provide crucial insights into surface complexity and heterogeneity, which are central to gas storage capacity. This CO_2-based fractal analysis is complemented by N_2 adsorption to evaluate mesopore structures, enabling a comprehensive assessment of pore complexity, roughness, and heterogeneity that are critical in applications such as methane recovery in CBM and CO_2 sequestration.

2. MATERIALS AND METHODS

2.1. Coal Sample Descriptions. A total of five coal samples each from a different coal mine in the Raniganj and Jharia Basins, India, with different thermal maturation histories were selected for this study. Sample CV-C was Jhama coal (i.e., with high ash, low volatile matter, high fixed carbon, and thermally metamorphosed due to the impact of igneous intrusion) collected from CV mines on the western part of the Raniganj Basin. Sample SB-C was collected from the Sonepur Bazari opencast mine located in the eastern region of the Raniganj Basin and is a high volatile bituminous coal of rank C.[33] Samples MK-C and MB-C were from the Mugma area in the western part of the Raniganj Basin and are also high volatile bituminous coal of rank A. Sample MO-C was collected from the Moraidih open cast mine in the Jharia Basin, from which coking coal is extracted, and is a medium volatile coal of rank Mvb. All of the mines from where the samples were collected (Raniganj and Jharia Basins) belong to the Damodar Valley Coal Province, India.

2.2. Petrographic Analysis. Petrographic analysis was performed on samples crushed to a size of 1.18 mm. A hot-mounting method for the preparation of pellets involved the applications of carnauba wax plus nigrosine in powdered form. The prepared pellets were polished adhering closely to the specifications of the ISO 7404−2[34] standard, ensuring that a scratch-free surface was generated. An optical microscope (Zeiss-AX10 model) was employed to conduct reflectance measurements and component-maceral analysis with a 50× magnification and oil-immersion objective lens. These measurements and analysis were performed by adhering closely to the ISO 7404−5[35] and ISO 7404−3[36] standards, respectively. Fluorescent blue light imaging was applied using an excitation filter (450−490 nm), a beam splitter (510 nm), and a barrier filter (515 nm) in order to distinguish liptinite macerals in the studied samples. Sapphire (*R*o: 0.589%), yttrium−aluminum−garnet (YAG: *R*o: 0.893%), and gadolinium−gallium−garnet (GGG: *R*o= 1.712%) were used for calibrations of normal coal samples for measuring the random vitrinite reflectance. Similarly, mean maximum reflectance measurement (*R*max) for the Jhama coal was taken by calibrating YAG, GGG, and cubic zirconia (*R*o: 3.14%) under crossed-polar.

2.3. Rock-Eval Analysis. Coal samples crushed to 212 μm sizes were used to determine their source rock properties using Rock-Eval 6. Rock-Eval's "basic/bulk-rock method" was employed for sample analysis, setting the final oxidation temperature at 750 °C.[37−40] This analysis yielded geochemical parameters, including total organic carbon (TOC, wt %), along with *S*1, *S*2, *S*3, *S*4, and T_{max} values. The full methodology can be found in previous studies by Carvajal-Ortiz and Gentzis[41] and Hazra et al.[39,40]

2.4. Low-Pressure Gas Adsorption. Pore structure, including surface area, pore volume, and pore size distribution, was investigated using a low-pressure gas adsorption (LPGA) technique. The samples were ground to a particle size of 212 μm and used in both nitrogen (N_2) and carbon dioxide (CO_2) adsorption experiments. Before the analysis, the samples were subjected to degassing at 110 °C for a duration of 3 h.[42,43] A Quantachrome Autosorb iQ instrument was employed for the analysis using N_2 and CO_2 as adsorbates. Throughout the experiment, the adsorbate's relative pressure (P/P_0) was progressively elevated until it attained the condensation pressure, which is specific to the temperature and intermolecular forces of the adsorbate. Here, P_0 represents the condensation pressure of the adsorbate, while P is the saturation pressure at each corresponding pressure point.

https://doi.org/10.1021/acs.energyfuels.5c00021
Energy Fuels 2025, 39, 5818−5831

Table 1. Rock-Eval Geochemical Properties of the Five Studied Indian Coal Samples[a]

basin/formation/age	sample ID	$S1$	$S2$	T_{max}	$S3$	PC	RC	TOC	HI	OI	$S4$
Raniganj/Barakar/Lower Permian	CV-C	1.26	25.82	443	1.60	2.43	69.77	72.20	36	2	610
Raniganj/Raniganj/Upper Permian	SB-C	1.24	106.22	429	10.12	9.9	56.70	66.6	159	15	520
Raniganj/Barakar/Lower Permian	MK-C	1.47	128.33	443	0.49	10.98	48.96	59.94	214	1	553
Raniganj/Barakar/Lower Permian	MB-C	1.54	116.13	445	1.11	10.04	54.80	64.84	179	2	568
Jharia/Barakar/Lower Permian	MO-C	0.66	82.64	472	2.15	7.19	58.09	65.28	127	3	577

[a]$S1$, $S2$: mg HC/g rock; T_{max}, $S4$: °C; $S3$: mg CO_2/g rock; PC, RC, TOC: wt %; HI: mg HC/g TOC; OI: mg CO_2/g TOC.

2.4.1. Low-Pressure N_2 Gas Adsorption. The LPGA analysis with N_2 was conducted on coal samples at a temperature of 77 K and a saturation pressure of 1 bar. A total of 40 data points were collected over a pressure range (P/P_0) from 0.01 to 0.99. N_2 adsorption isotherms were used to analyze the mesopore size distribution (PSD), surface area, and Frenkel−Hasley−Hill (FHH) fractal dimensions (D). The FHH method for extracting D values is widely applied.[44] It is common to consider two fractal component parts relating to an isotherm, $D1$ and $D2$.[21,45] Mesopore diameters between 2 and 8 nm tend to become gas-saturated within the lower relative pressure interval (0.01−0.5) of the isotherm with van der Waals forces playing a key role; fractals extracted from that interval are referred to as the $D1$. Mesopore diameters between 8 and 50 nm tend to become gas-saturated within the upper relative pressure interval (0.5−0.99) by capillary condensation; extracted from that interval are referred to as the D2. The specific surface area (SSA) was analyzed using the multipoint Brunauer−Emmett−Teller (BET) equation, while the PSD was computed using the Barrett−Joyner−Halenda (BJH) model. The full experimental procedure is detailed in Ross and Bustin[46] and Kuila and Prasad.[47]

2.4.2. Low-Pressure CO_2 Gas Adsorption. CO_2-based LPGA experiments on coal samples were performed in a water bath, with the temperature consistently maintained at 273 K. The relative pressure range (P/P_0) for these experiments spanned from 0.0005 to 0.03. CO_2 adsorption isotherms were employed to analyze the micropore volume and surface area, utilizing the Dubinin−Astakhov (DA) and Dubinin−Radushkevich (DR) equations, respectively.[48,49] Graphical analysis to determine adsorption potential (β) was conducted by plotting $\ln(Q)$, representing the adsorbed gas quantity, against ε^2, the Polanyi potential. The micropore surface area (S_{micro}) and micropore volume was determined using the following equations:[48,49]

$$S_{micro} = \frac{1}{4}\pi\beta^2 \tag{1}$$

$$V_{mic} = \frac{V_0}{2}\int_0^{\ln\left(\frac{P}{P_0}\right)} e^{\beta\varepsilon^2} d\ln(P/P_0) \tag{2}$$

where V_0 represents a material constant, β corresponds to the adsorption potential, ε denotes the characteristic energy of adsorption, and P/P_0 signifies the relative pressure. The micropore volume is obtained by integrating the natural logarithm of the pressure ratio, which is derived from the adsorption isotherm data. Micropore size distribution was analyzed using the density functional theory (DFT) method.[50] This approach is based on molecular statistical thermodynamics, which calculates the amount of adsorbed gas within a specific pore size range under the given experimental conditions of temperature and pressure. The calculation involves solving the equation for the grand thermodynamic potential, which describes how the gas density is distributed within the pore structure. To calculate micropore fractal dimensions, CO_2 isotherms were analyzed using three different fractal models: DR, FHH, and Mandelbrot pore volume versus cumulative surface area (V−S) models.

3. RESULTS AND DISCUSSION

3.1. Geochemical Properties and Organic Petrology.

Table 1 presents the Rock-Eval results, and Figure 1 displays the photomicrographs of the studied coals. Sample SB-C from the Sonepur Bazari area of the Raniganj Basin is identified as the least thermally mature coal (T_{max}: 427 °C; classified as thermally immature) of the studied samples. In addition, the lowest VRo coal SB-C also has a higher vitrinite content. In general, coals from the eastern part of the Raniganj Basin, India, are "noncoking" and characterized as high volatile bituminous C rank.[32] vitrinite reflectance (Ro) for sample SB-C is 0.58% (Table 2), placing it close to the "first coalification jump". In contrast, the coals MK-C and MB-C from the Mugma and Bajdna areas of the western part of the Raniganj Basin are marked by higher T_{max} (443 and 446 °C, respectively) and vitrinite reflectance (0.81 and 0.89%, respectively), placing them close to the "peak oil window" and "second coalification jump".

Sample MK-C exhibits the highest HI and the highest liptinite content (12.5 vol %; mmf basis) among the studied suite of samples. Sample MO-C, collected from the Moraidih mines of the Jharia Basin, recorded the highest thermal maturity level in terms of measured T_{max} of 472 °C and Ro of 1.31%, indicating it to be at the post thermal maturity level close to the "third coalification jump". vitrinite (61.3 vol %) constitutes the dominant maceral within this coal, which are also characterized by the absence of liptinites.

The Jhama coal sample CV-C collected from the Chanch Victoria mines of the Raniganj Basin (western part of the basin) has the lowest HI value. The influence of a nearby igneous intrusion caused volatiles and hydrocarbons to be expelled from this sample, resulting in its low HI value. Petrographic investigation of the sample also recorded a high proportion of thermally altered material within CV-C (Figure 1). Due to the impact of intrusion, as hydrocarbons/volatiles are eliminated from the system, the residual organic matter present in the sample becomes highly aromatized. However, the T_{max} from Rock-Eval analysis of this sample is only 443 °C, classifying it as "early mature". The Ro (max and min) for the CV-C coal varies between 0.50 and 2.89 with a bireflectance of 2.39. A typical bireflectance range of 0.20 to 6.21 is commonly reported for heat-affected coal, coke, and burnt coke.[51] The bireflectance observed in this study is similar to that of heat-altered coal.

Analyzing, the Rock-Eval S2 (pyrolyzates generated from the breakdown of organic matter during pyrolysis and generated by the flame ionization detector) and $S4CO_2$ (CO_2 generated from the combustion of organic matter during the oxidation phase and detected by the IR detector) curves clarified the cause of this inconsistency. While bell-shaped smooth S2 curves were observed for the other coal samples studied (Figure 2A−E), for the Jhama coal CV-C the S2 curve is bimodal, making it unreliable for T_{max} analysis. Hazra et al.[33] noted similar problems, i.e., unreliable T_{max} for heat-altered shales, and observed Rock-Eval $S4$-T_{peak} to be more effective for determining thermal maturity levels of such samples. Figure 2A'−E' shows the disposition of the $S4CO_2$ curve of the studied coals. Similar to $S2$ T_{max}, the $S4$-T_{peak} value systematically increases from the thermally immature SB-C sample (520 °C) to the peak oil window samples MK-C (553 °C) and MB-C (568 °C) to the postmature MO-C sample (577 °C). Moreover, the

https://doi.org/10.1021/acs.energyfuels.5c00021
Energy Fuels 2025, 39, 5818−5831

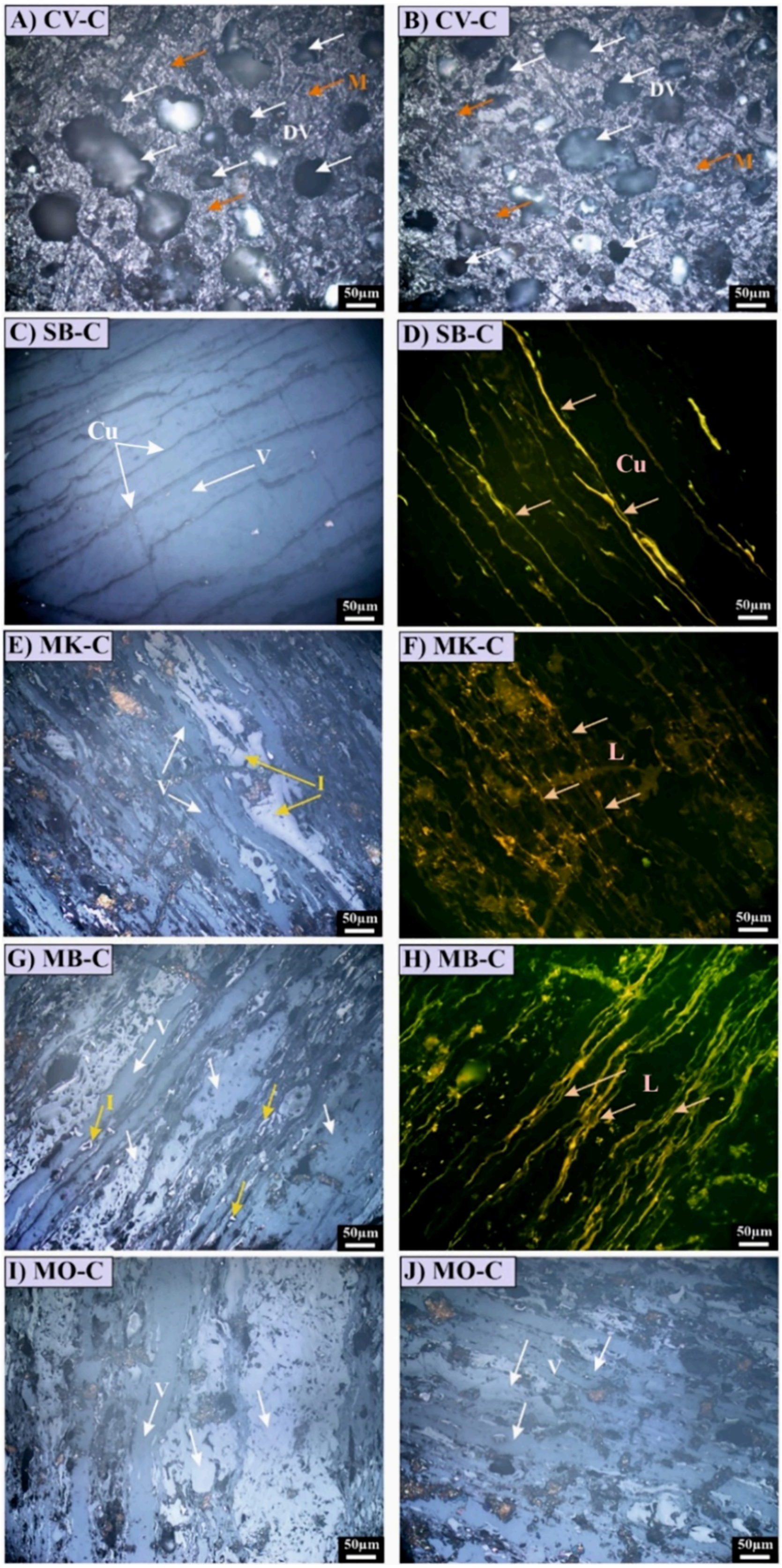

Figure 1. Microphotographs of CV-C (A, B), SB-C (C, D), MK-C (E, F), MB-C (G, H), and MO-C (I, J) coal samples. Abbreviations: DV - Devolatilized vacuoles; M - Mosaics; V - vitrinite; L - Liptinite; Cu - Cutinite; I - Inertinite.

highest $S4\text{-}T_{peak}$ value (610 °C) was noted for the Jhama sample CV-C, more realistically reflecting the higher thermal maturity level of the sample, caused by the impacts of igneous intrusion. The more aromatized structures of this metamorphosed sample

https://doi.org/10.1021/acs.energyfuels.5c00021
Energy Fuels 2025, 39, 5818−5831

Table 2. Petrographic Composition of the Studied Coals[a]

sample ID	V^{mmf} (vol %)	I^{mmf} (vol %)	L^{mmf} (vol %)	*Ro* (%)
CV-C[b]	3.5	31.5	0	2.89[c]
SB-C	70.5	20.0	9.5	0.58
MK-C	56.0	31.5	12.5	0.81
MB-C	53.5	40.5	6.0	0.89
MO-C	61.3	38.7	0	1.31

[a]V - vitrinite; I - Inertinite; L - Liptinite; mmf: mineral matter free basis; *Ro* - vitrinite reflectance (%). [b]High percentage of heat-altered grains (65%). [c]Ro (max) of CV-C.

require higher temperatures for complete breakdown/reaction during the oxidation stage.[52]

3.2. Low-Pressure N_2 Adsorption. Table 3 presents the pore structural properties of the studied coals determined by using the LPGA technique. The BET SSA ranged from 1.35 to 3.07 m^2/g. Moreover, no relationship was evident between the N_2-derived BET SSA and the thermal maturity levels of the coal samples (Table 3). Figure 3 depicts the N_2-LPGA isotherms of the five coal samples used in this study. The overall shape of the N_2-LPGA isotherms provides insight into the pore network.[47] The International Union of Pure and Applied Chemistry (IUPAC) categorizes adsorption isotherms into six types, with a comprehensive classification available in the works of Sing[9] and Rouquerol et al.[53] The low-pressure nitrogen adsorption−desorption isotherms of the coals in this study exhibit distinct hysteresis patterns, a clear indication of capillary condensation occurring within the mesopores. However, contrary to what one might expect from type IV isotherms, which typically feature a plateau at high relative pressures—signifying the completion of mesopore filling—the samples do not show such a plateau. Instead, the isotherms present steep slopes at elevated relative pressures, indicating the existence of macropores, as noted by Kuila and Prasad[47] and further corroborated by Hazra et al.[21,26] Rouquerol et al.[53] classified these isotherms as Type IIB, characterizing them by the coexistence of mesopores—responsible for the observed hysteresis—and macropores, which account for the absence of a plateau typical of Type IV materials. Thus, the adsorption isotherms for the samples studied were identified as Type IIB, as illustrated in Figure 3.

In general, the BJH pore volume and average pore diameter of the coals were observed to vary between 0.003 and 0.004 cc/g and 6.10 and 10.79 nm, respectively, with the coal rank showing no visible impact on the pore structural parameters. The pore size distributions of the coals obtained using the BJH adsorption model are presented in Figure 4. The pore volumes within the smaller size interval (∼10 nm) were the largest for the high-volatility bituminous rank C SB-C coal sample. This corroborates with the higher BET SSA and lowest pore diameter recorded for the SB-C coal compared to the other coal samples. The nitrogen gas adsorption-derived fractal dimensions (*D*1 and *D*2) calculated using the FHH model, also did not show any definitive trend with the rank of the coal samples (Table 3; Figure 3). Coal sample SB-C, the least thermally mature among the studied suite, showed the highest *D*2, while the coals that are higher in thermal maturity exhibited smaller values. On the other hand, *D*1 was observed to be least for SB-C, while the Jhama sample (CV-C) had highest *D*1 (Table 3). The nonsystematic variations in the pore properties of the studied coals could be due to their individual properties; however, they may also suggest certain complexities in comprehending their pore structural characteristics.

It is necessary to take into account that the low-pressure N_2 gas adsorption technique is associated with uncertainties when applied to extremely organic-rich (TOC > 10 wt %) shales and coals.[17] Several researchers have reported that the N_2 gas adsorption-derived SSA is substantially lower than the CO_2 gas adsorption-derived SSA in wide range of coal samples.[54−59] This could be due to the fact that the CO_2 gas adsorption-derived SSA comprises a substantial micropore contribution in its SSA values. A strong case can be made that N_2 and CO_2 gas adsorption isotherm analysis should not be compared, as they are not measuring the same parts of the pore network present in the organic minerals of such samples or even overlap in the observed pores. This being said, N_2 adsorption data measures mainly the mesopores, whereas the CO_2 adsorption data measures micropores.

An additional problem is that N_2 at experimental conditions (−196 °C) exhibits low kinetic energy, which inhibits its ability to penetrate the complex micropore networks of coals, particularly as some of those pores shrink at such low-temperature conditions.[26,57,60,61] The pore networks of coals behave as molecular sieves with respect to N_2, with molecules limiting their entry into pores with diameters less than about 4 Å, whereas CO_2 molecules can penetrate much smaller-sized pore spaces.[62−64] These factors potentially explain the apparent reduction in pore-scale surface areas derived from the N_2 adsorption isotherms in certain coals. Therefore, it is worthwhile to compare the surface area and fractal dimensions determined from N_2 and CO_2 adsorption isotherms from the same coal samples displaying a range of thermal maturities. Such comparisons could potentially distinguish between genuine pore structural variations that may occur in coals, as they become more thermally mature and free from limitations in N_2 adsorption analysis of the pore network, especially in coal samples that are very complex.

3.3. Low-Pressure CO_2 Adsorption. Table 4 lists the results of the CO_2 adsorption experiments. Figure 5 shows the CO_2 adsorption isotherms of the studied coals. All the samples showed development of a Type I isotherm with a greater adsorption rate at the lower relative pressures, indicating the presence of micropores. Moreover, the lowest adsorption capacity was shown by the lowest rank coal SB-C (high volatile, bituminous coal of rank C). The two coals MK-C and MB-C representing high volatile bituminous rank A showed nearly similar adsorption capacities, with sample MB-C showing a marginally higher volume than MK-C. Interestingly, sample MO-C (medium volatile rank Mvb) showed the highest adsorption capacity. Sample CV-C, despite having the highest $S4\text{-}T_{peak}$, showed a substantially smaller CO_2 adsorption capacity than MO-C (but has a substantially higher volume than the other samples), indicating possible destruction of some micropores within the sample due to the impact of igneous intrusion resulting from forceful/quickened expulsion of hydrocarbons from the sample due to the thermal stress induced by the igneous intrusion. Micropore size distributions calculated using the CO_2-based DFT model further corroborated the above findings (Figure 6), with the Mvb coal (MO-C) showing the largest volume of micropores across the entire size range (except between the size range of 0.75−0.85 nm, where the lowest rank SB-C coal showed the highest concentration of pores). Consequently, the higher micropore surface area and micropore volume were noted in sample MO-C, followed by the thermally altered CV-C sample and the least being shown by sample SB-C.

https://doi.org/10.1021/acs.energyfuels.5c00021
Energy Fuels 2025, 39, 5818−5831

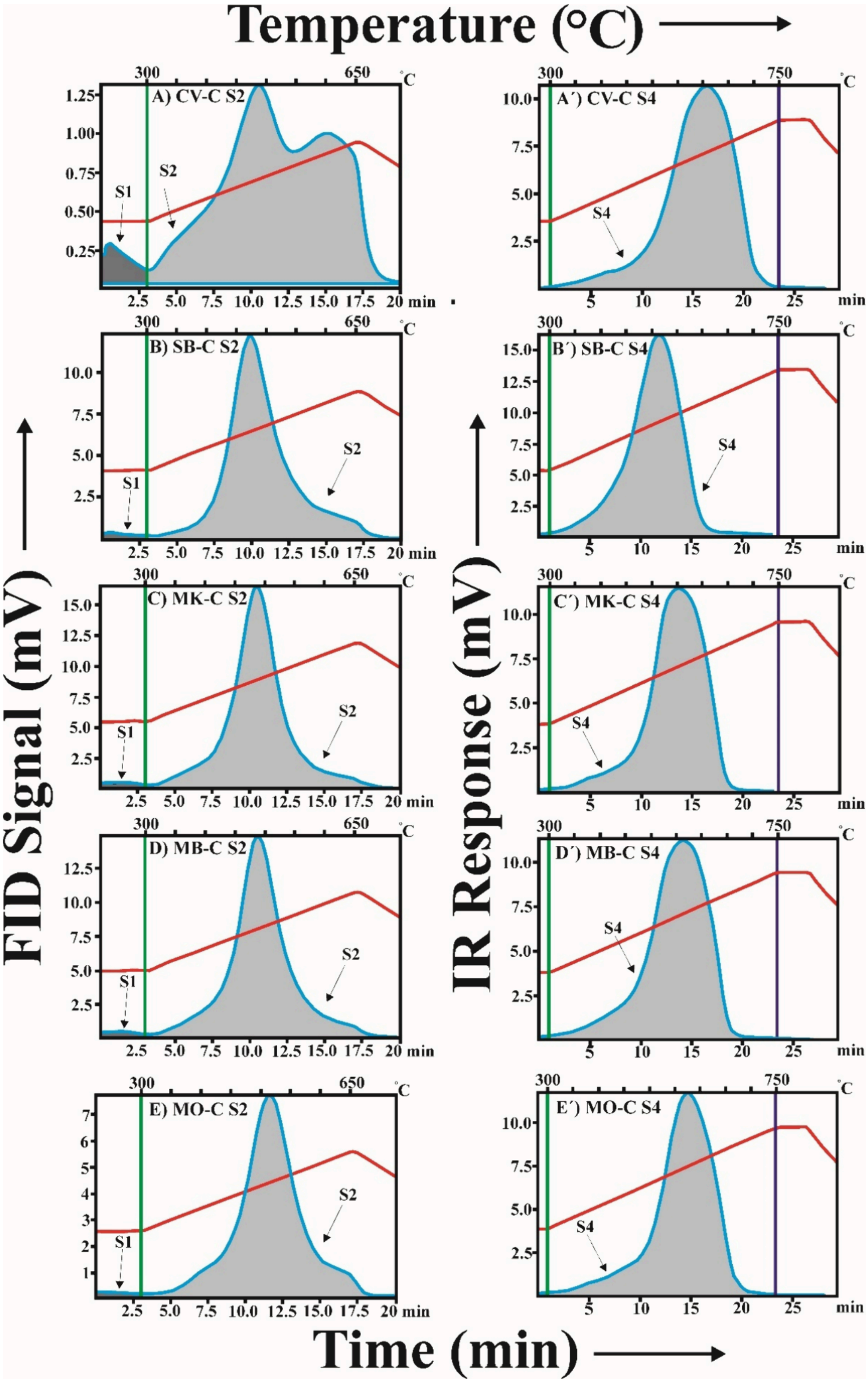

Figure 2. $S2$ pyrograms and $S4$-CO_2 oxidation graphics of CV-C (A, A'), SB-C (B, B'), MK-C (C, C'), MB-C (D, D'), and MO-C (E, E') coal samples.

Table 5 presents the fractal dimensions calculated from the CO_2 adsorption isotherms recorded for the five coal samples based on three distinct fractal calculation methods, namely, Dubinin−Radushkevich (DR), Frenkel−Halsey−Hill (FHH), and Mandelbrot pore volume versus cumulative surface area (V−S) model.[65]

The DR fractal calculation method considers the theory of pore filling and the relationship expressed in eq 3[46,66]

$$\log V = \log(V_0) - C\log^2\left(\frac{P}{P_0}\right) \quad (3)$$

where V is the volume of adsorbed gas at equilibrium pressure, V_0 is the total micropore volume, P is the pressure, $P0$ is the saturation vapor pressure, and C is a constant. The linear negative slope of relationship $\log(V/V0)$ versus $\log^2(P/P0)$

Table 3. Pore Structural Parameters Determined by a Low-Pressure Adsorption Technique Using N_2 as the Adsorbate

sample ID	average pore diameter (nm)	BJH pore volume (cc/g)	BET SSA (m^2/g)	*D*1	*D*2
CV-C	8.60	0.004	1.95	2.27	2.72
SB-C	6.10	0.004	3.07	2.06	2.80
MK-C	10.79	0.003	1.35	2.15	2.67
MB-C	9.80	0.004	1.70	2.23	2.68
MO-C	9.45	0.004	1.61	2.11	2.70

represents the energy of adsorption. The fractal dimension of the microporosity (D) is derived as 3 plus that negative slope.[46,66]

The $V-S$ method considers the positive, near-linear relationship between the cumulative pore volume (V) and the cumulative specific surface area (S) of the porous samples as expressed by eq 4.[65,67]

$$\ln V = \left(\frac{3}{D}\right)\ln S + C \tag{4}$$

D is derived from eq 4 as three divided by the slope of the line defined by a cross plot of ln V versus ln S.[67]

The graphical relationships used to derive the fractal dimension for each of the coal samples from the recorded CO_2 adsorption isotherms are displayed in Figure 7, where the plots A−E are for the DR method and plots F−J are for the $V-S$ method.

Unlike N_2 molecules, the CO_2 molecule is for the most part absorbed to fill pores/micropores in porous media without involving capillary condensation.[68] As the FHH fractal calculation model involves multilayer-adsorption assumptions, it is typically considered inappropriate for the interpretation of CO_2 adsorption isotherms.[9,67] Nevertheless, the FHH method is applied to the studied samples to compare the fractal dimension

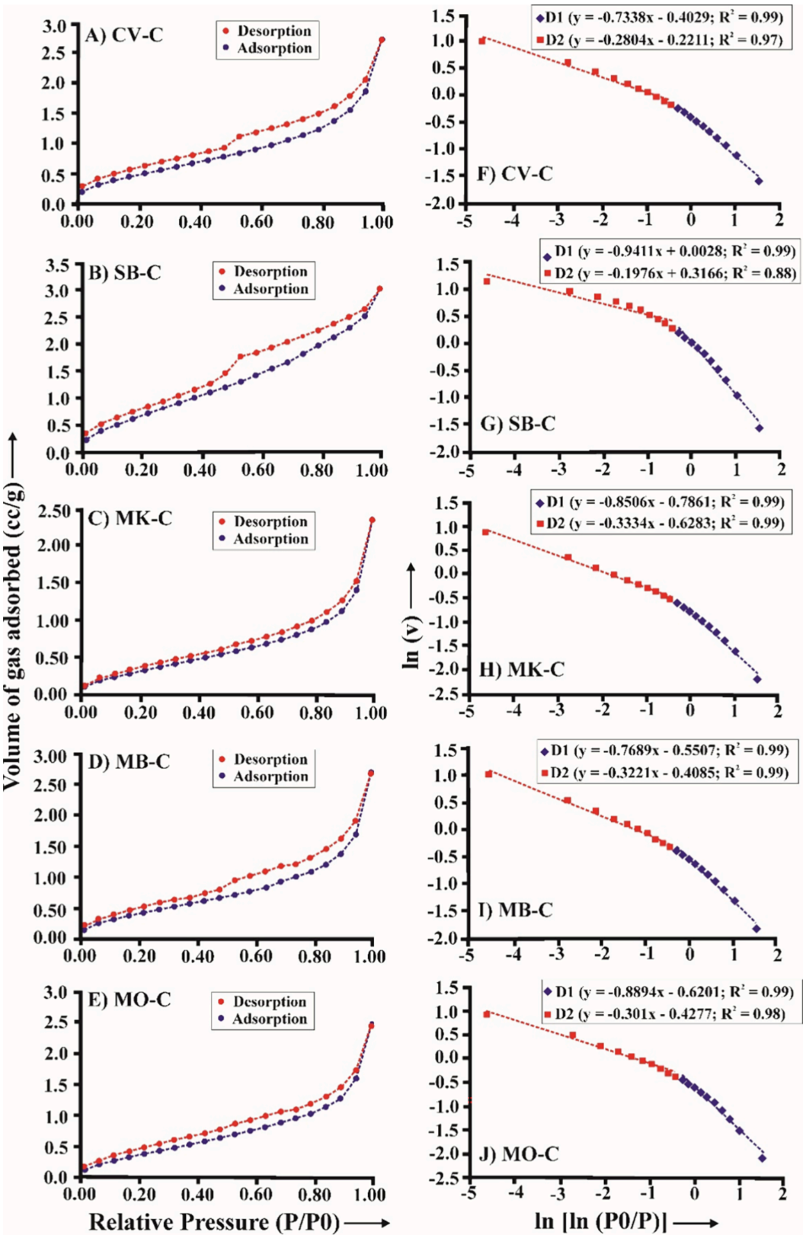

Figure 3. Low-pressure N_2 adsorption−desorption isotherms (A−E) and FHH fractal dimension plots (F−J) of the studied coals.

https://doi.org/10.1021/acs.energyfuels.5c00021
Energy Fuels 2025, 39, 5818−5831

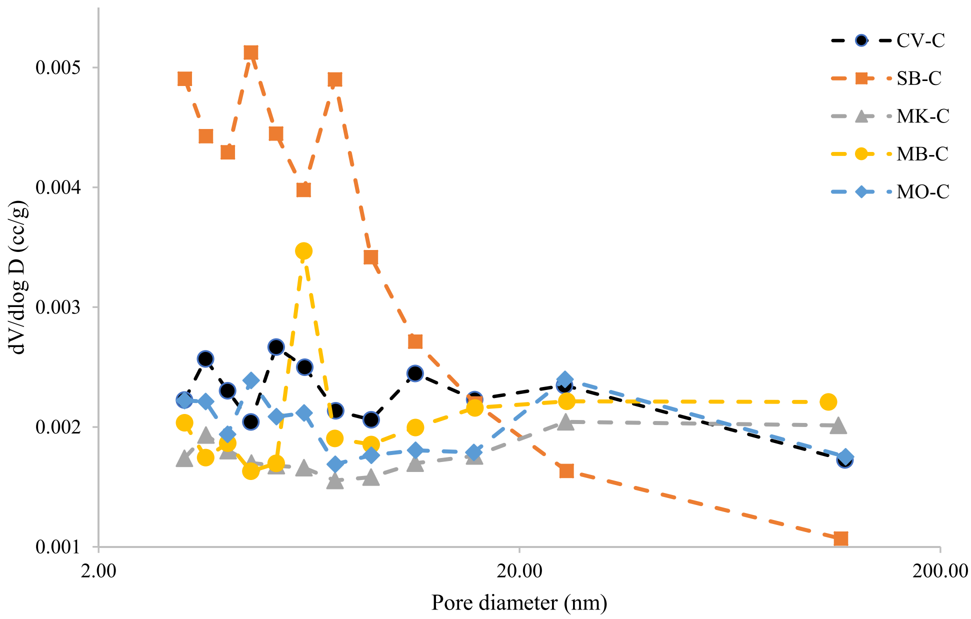

Figure 4. PSD plots of the five studied coal samples determined using the BJH adsorption model.

Table 4. Pore Structural Parameters Derived from CO_2-LPGA Isotherm Analysis

Sl. no.	D − R micropore surface area (m^2/g)	D − R micropore volume (cc/g)	D − R pore width (nm)	D − A micropore volume (cc/g)	D − A pore diameter (nm)	DFT surface area (m^2/g)	DFT pore volume (cc/g)
CV-C	121.571	0.048	0.908	0.065	1.380	114.700	0.036
SB-C	80.734	0.030	0.942	0.056	1.460	64.431	0.020
MK-C	95.699	0.036	0.960	0.068	1.480	80.870	0.026
MB-C	93.755	0.035	0.942	0.065	1.46	78.335	0.024
MO-C	155.11	0.058	0.928	0.071	1.380	137.544	0.044

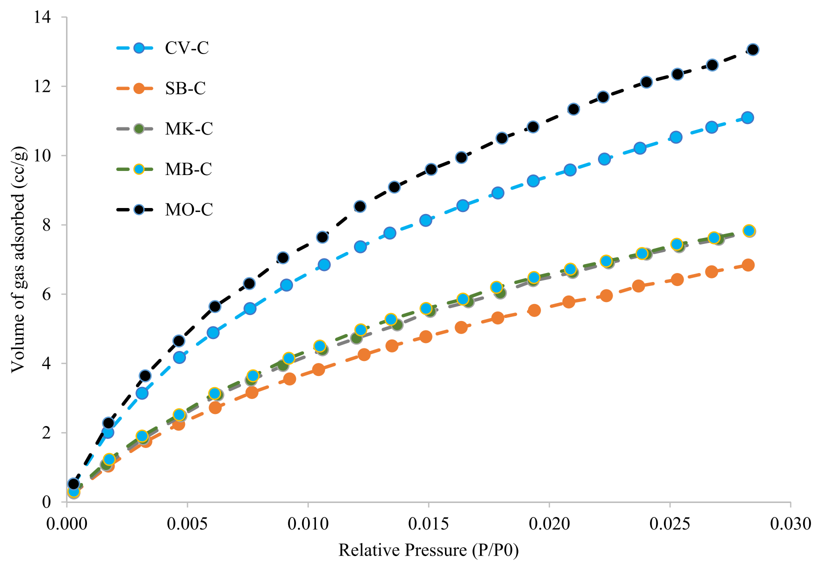

Figure 5. CO_2 gas adsorption isotherms of the studied coals.

trends with those generated by the DR and $V-S$ methods, which are more generally accepted as suitable for CO_2 adsorption isotherm fractal analysis. Another challenge with the FHH method is that it generates nonlinear curves for ln V versus $\ln[-\ln(P0/P)]$ trends introducing uncertainties into the slopes fitted to those trends. For this reason, in addition to calculating FHH using the complete isotherm data (FHH*), fractal dimensions are calculated with the first half (FHH $D1$) and the second half (FHH $D2$) of the isotherm, for which less nonlinearity trends exist for most samples. Despite the FHH*, $D1$, and $D2$ calculated fractals having distinctive value ranges (Table 4), highlighting the uncertainty with this method, their value distributions show strong positive correlations with each other. Hence, for graphical comparison with the other CO_2 adsorption isotherm fractal calculation methods, the FHH*

https://doi.org/10.1021/acs.energyfuels.5c00021
Energy Fuels 2025, 39, 5818−5831

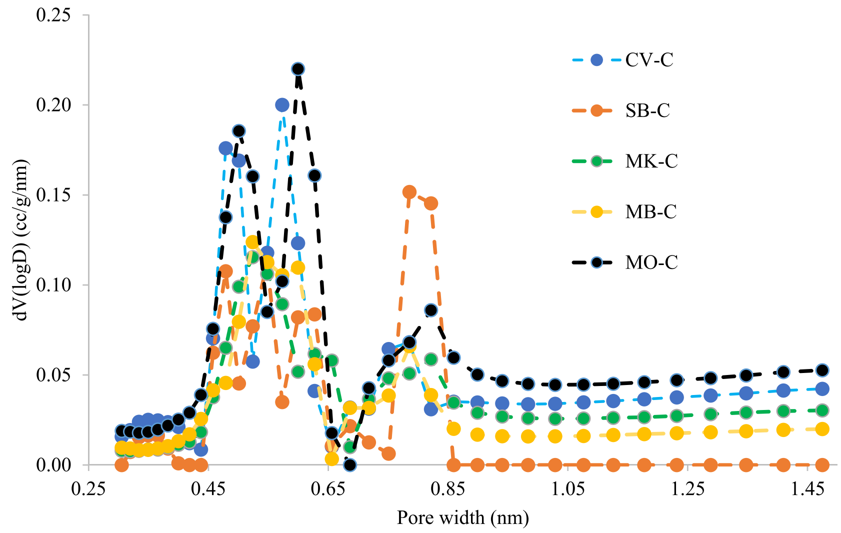

Figure 6. Micropore size distributions for the X series (A and B) and Y series (C and D) samples calculated using the CO_2-based DFT model.

Table 5. Calculated Fractal Dimensions from the CO_2 Adsorption Isotherms[a]

coal sample	DR	FHH*	FHH $D1$	FHH D2	V−S
CV-C	2.867	2.692	1.626	2.946	2.608
SB-C	2.857	2.664	1.550	2.442	2.523
MK-C	2.851	2.651	1.482	2.938	2.505
MB-C	2.857	2.665	1.534	2.941	2.490
MO-C	2.861	2.678	1.564	2.946	2.487

[a]FHH* refers to calculations involving the entire isotherm; FHH $D1$ involves the sector of the isotherm with $P/P0$ values <0.5; FHH $D2$ involves the sector of the isotherm with $P/P0$ values ≥0.5.

values are used as the most reliable ones for further interpretation of the data (Figure 8).

Figure 9 displays the calculated fractal dimension from each of the three methods versus Rock-Eval $S4$ peak T_{max} and HI values. It is apparent that the DR and FHH* display clear and similar trends to $S4$ T_{max} and HI for the five samples, although the FHH*-calculated fractal dimension values are approximately 0.2 lower than the DR-calculated values. There is a strong positive correlation between both DR and FHH* fractal dimensions and $S4$ T_{max} (Figure 9A,C), and a strong positive relationship between those two calculated fractal dimensions and HI (Figure 9B,D). Coal sample MK-C, with the highest liptinite content (Table 2), is associated with the lowest fractal value and the largest HI value, and the metamorphosed coal sample (displaying the highest thermal maturity), CV-C, is associated with the highest fractal value and lowest HI value (Figure 9). However, the trends between the fractal dimensions calculated by the V−S method are less correlated with the $S4$ T_{max} (Figure 9E,F). In particular, coal samples MO-C and MB-C are associated with the lowest V−S fractal values, although sample CV-C is still distinguished with the highest fractal values.

It is noticeable in Figure 9, with all three calculated fractal dimension values (Figure 9A−E), that the least thermally mature sample, SB-C, lies off-trend compared to the other coal samples. A comparison of the CO_2 isotherm-derived pore size distributions of the five coals reveals that coal SB-C has a distinctive pore size distribution from the other coals, being dominated by nanopores of diameter ∼0.8 nm rather than the smaller 0.4−0.6 nm range. This could be partly responsible for its off-trend position in Figure 9A,C. However, this may also be due, at least in part, to its distinctive petrographic composition.

In general, the fractal dimension analysis of the five coal samples revealed significant influences from thermal maturity, organic petrology, and kinetic distributions, demonstrating the complexity of pore networks and their evolution across varying coal ranks. Thermally mature and postmature coals exhibited higher fractal dimensions, reflecting enhanced micropore network development and surface heterogeneity, while maceral composition played a key role in shaping these attributes. Liptinite-rich coals displayed simpler pore structures, whereas vitrinite-rich and heat-altered coals exhibited more complex networks, underscoring the interplay between organic composition and the degree of thermal maturity. However, this study is based on a limited set of samples, and further research is necessary to validate these findings. Future work should include a larger data set encompassing a broader range of coals, particularly immature and mature samples with diverse organic petrology. An expanded sample set featuring coals dominated by specific macerals (vitrinite, liptinite, and inertinite) would help establish whether distinct differences in fractal dimensions exist among these coal types, providing deeper insights into the factors governing pore complexity and the gas storage potential of specific coal types.

■ CONCLUSIONS

This study investigated the pore structural complexities and gas storage potential of thermally contrasting Indian coals by using low-pressure nitrogen (N_2) and carbon dioxide (CO_2) adsorption techniques. Fractal dimensions were calculated from CO_2 adsorption data using the Dubinin−Radushkevich (DR), Frenkel−Halsey−Hill (FHH), and Mandelbrot pore volume versus cumulative surface area (V−S) models to comprehensively evaluate micropore complexity and heterogeneity and relate it to thermal maturity and organic petrology. Based on the results, the following conclusions are drawn:

- Thermal maturity significantly influences the pore structure of coals, with postmature coals displaying greater micropore volumes and higher fractal dimensions. These properties suggest that increased thermal maturity enhances surface complexity and gas storage capacity,

https://doi.org/10.1021/acs.energyfuels.5c00021
Energy Fuels 2025, 39, 5818−5831

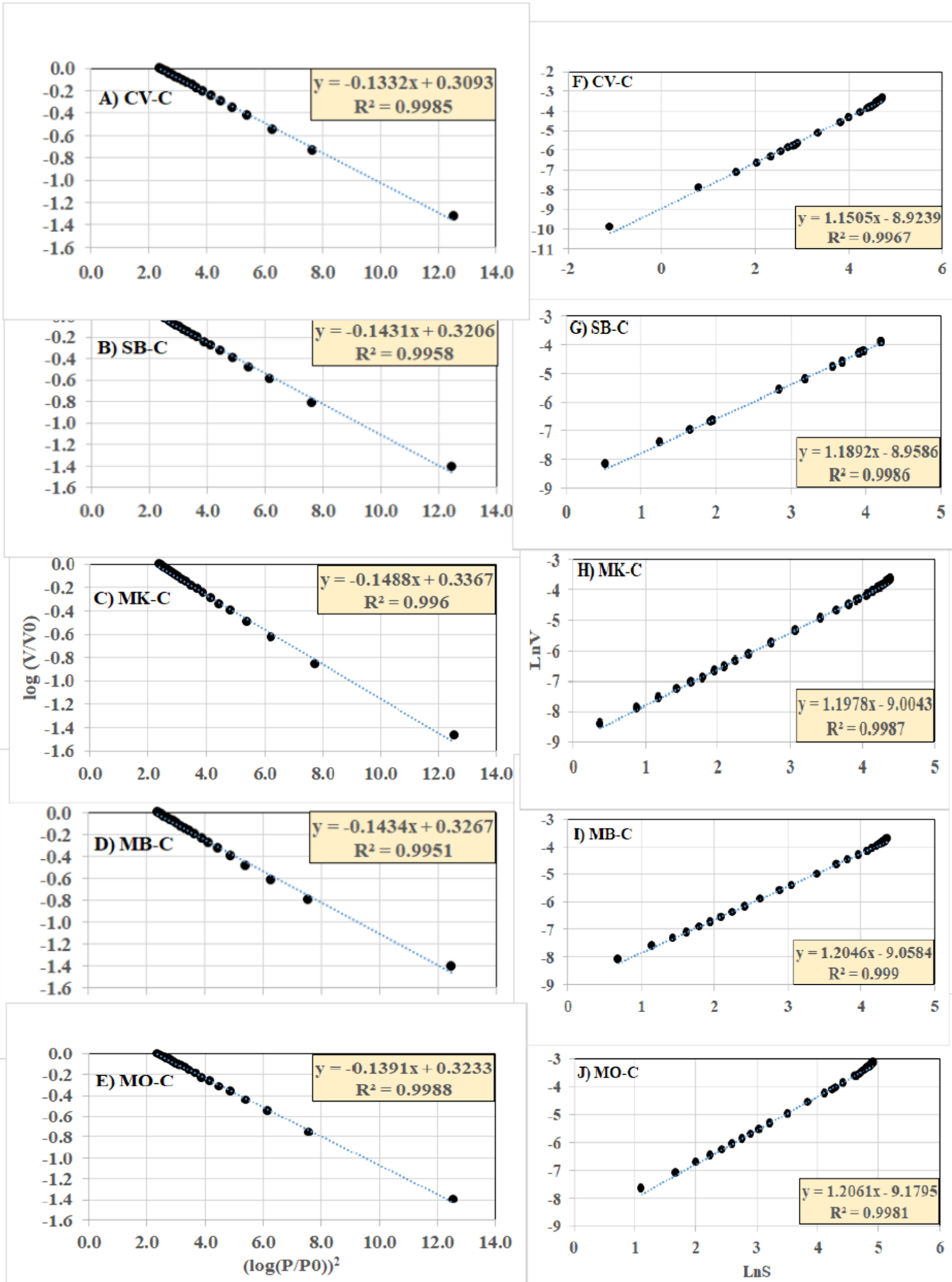

Figure 7. Low-pressure CO_2 adsorption fractal calculations for the five studied coal samples. (A–E Dubinin–Radushkevich (DR) model; (F–J) Mandelbrot pore volume versus cumulative surface area (V–S) model.

making such coals more favorable for applications such as CBM extraction and CO_2 sequestration.

- The CO_2 adsorption method provided a more comprehensive understanding of micropore structures compared to N_2 adsorption. CO_2-derived micropore surface areas ranged from 80.73 m^2/g (SB-C) to 155.11 m^2/g (MO-C), significantly higher than the N_2-derived BET surface areas (1.35–3.07 m^2/g).
- Fractal analysis revealed strong correlations between pore complexity and thermal maturity markers. Postmature coals with higher $S4$ T_{max} values, such as CV-C (610 °C) and MO-C (577 °C), exhibited the most complex pore structures, as reflected in higher fractal dimensions across all models.
- The highest CO_2 adsorption-derived fractal dimensions were observed in postmature coal with higher vitrinite content (MO-C: 61.3 vol %) and heat-altered coal (CV-C: 65% thermally altered grains). Liptinite-rich coal (MK-C: 12.5 vol %) exhibited lower fractal dimensions, indicating a simpler pore structure.
- CV-C, affected by igneous intrusion, has a high thermal maturity ($S4$ T_{max}: 610 °C) but lower CO_2 adsorption capacity (0.048 cc/g) than MO-C (0.058 cc/g), indicating micropore damage due to thermal stress, which leads to increased surface complexity but reduced adsorption efficiency compared to nonintruded postmature coals.

https://doi.org/10.1021/acs.energyfuels.5c00021
Energy Fuels 2025, 39, 5818–5831

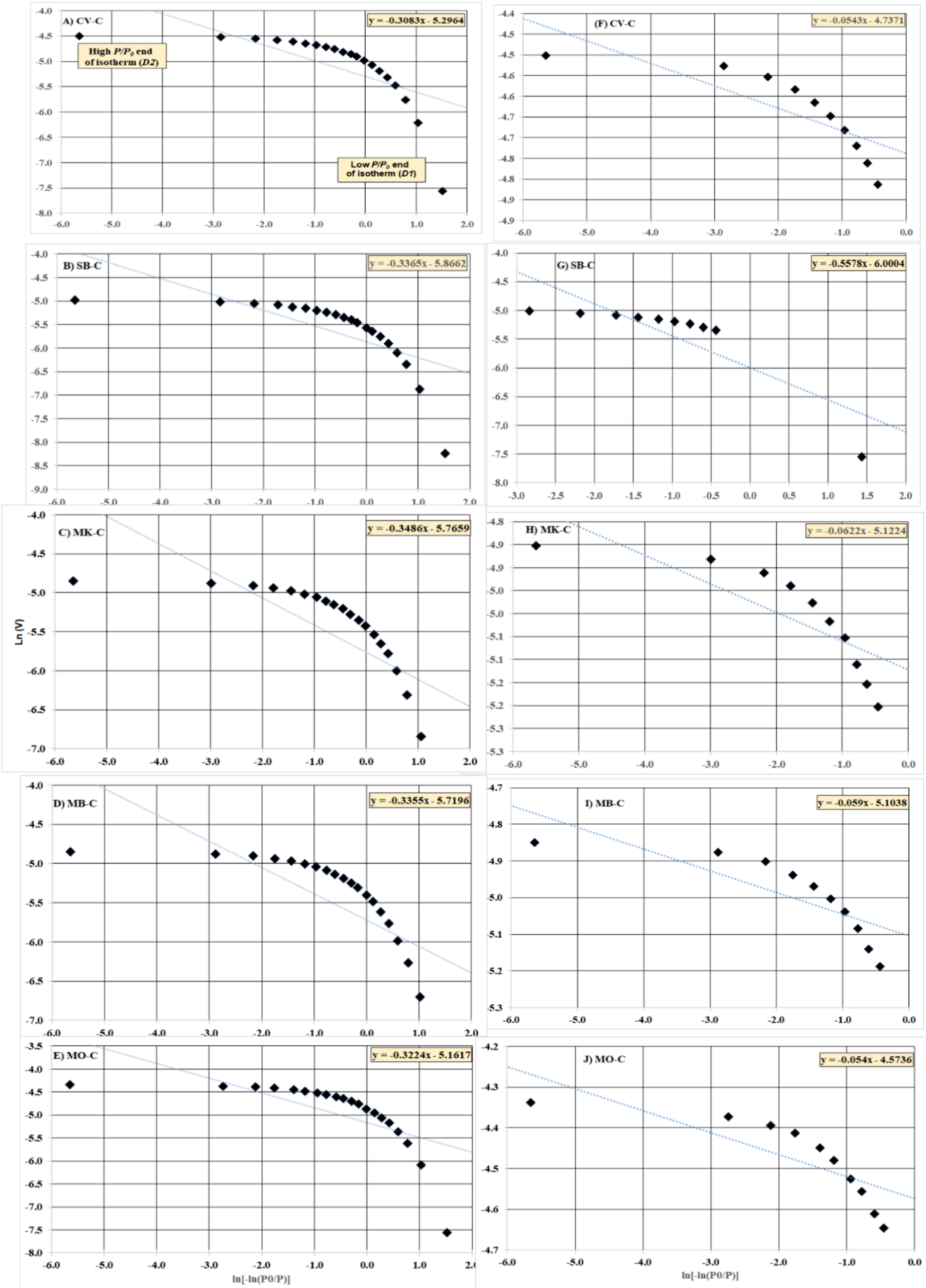

Figure 8. Low-pressure CO_2 adsorption fractal calculations for the five studied coal samples. (A−E) Frenkel−Halsey−Hill (FHH*) model applied to full isotherm; (F−J Frenkel−Halsey−Hill (FHH $D2$) model applied to the part of the isotherm with $P/P0$ values ≥0.5.

https://doi.org/10.1021/acs.energyfuels.5c00021
Energy Fuels 2025, 39, 5818−5831

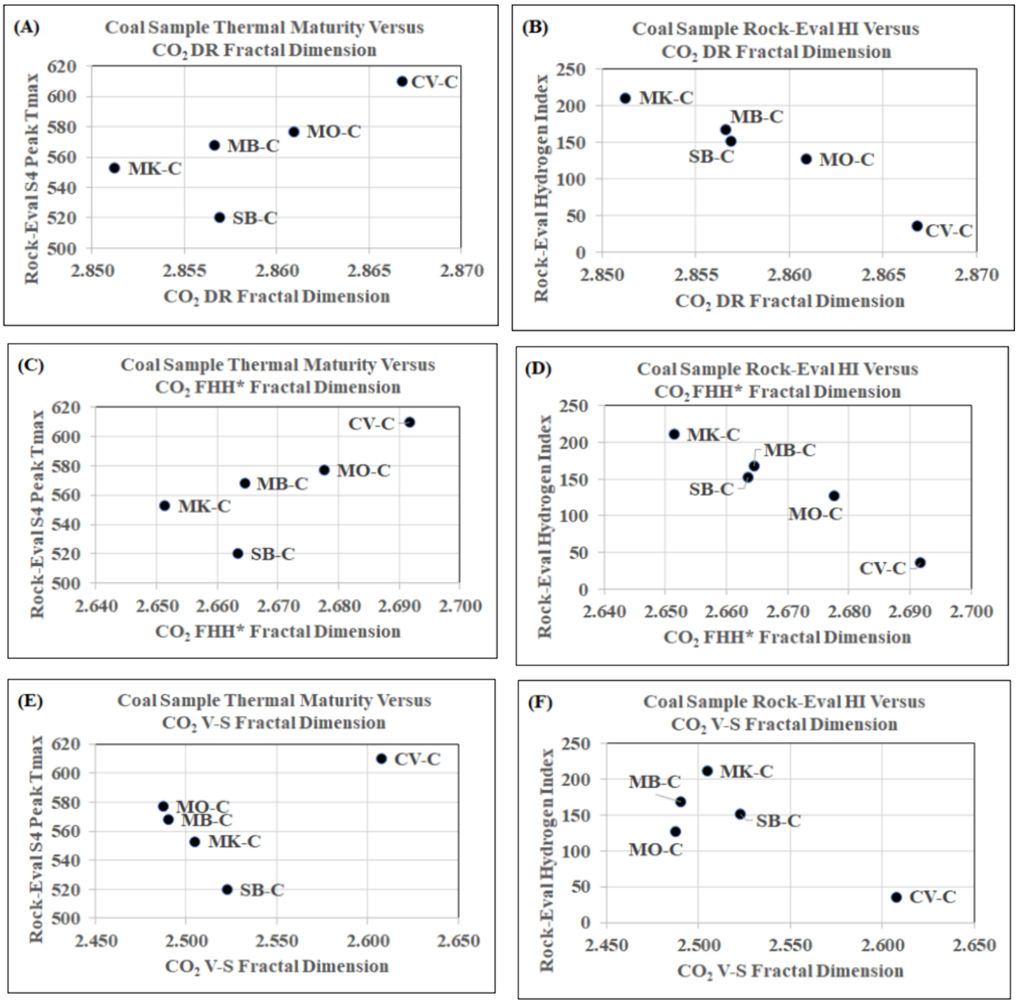

Figure 9. Fractal dimensions determined by three methods from CO_2 adsorption analysis compared with *S4* T_{max} and HI for the five studied coal samples: (A) DR vs *S4* T_{max}; (B) DR vs HI; (C) FHH* vs *S4* T_{max}; (D) FHH* vs HI; (E) *V*–*S* vs *S4* T_{max}; (F) *V*–*S* vs HI.

AUTHOR INFORMATION

Corresponding Authors

Bodhisatwa Hazra – *CSIR- Central Institute of Mining and Fuel Research, Dhanbad, Jharkhand 826001, India;* orcid.org/0000-0002-3462-7552; Email: bodhisatwa.hazra@gmail.com

Mehdi Ostadhassan – *Institute of Geosciences, Marine and Land Geomechanics and Geotectonics, Christian-Albrechts-Universität, Kiel 24118, Germany;* orcid.org/0000-0001-9235-4399; Email: mehdi.ostadhassan@ifg.uni-kiel.de

Authors

David A Wood – *DWA Energy Limited, Lincoln LN5 9JP, United Kingdom;* orcid.org/0000-0003-3202-4069

Mahima Panda – *CSIR- Central Institute of Mining and Fuel Research, Dhanbad, Jharkhand 826001, India*

Chinmay Sethi – *CSIR- Central Institute of Mining and Fuel Research, Dhanbad, Jharkhand 826001, India*

Vikram Vishal – *National Centre of Excellence in CCUS, Department of Earth Sciences, Indian Institute of Technology Bombay, Mumbai 400076, India;* orcid.org/0000-0001-6342-9603

Debanjan Chandra – *Department of Geoscience and Engineering, Delft University of Technology, Delft 2628 CN, The Netherlands; Department of Geosciences, Norwegian University of Science and Technology, 7031 Trondheim, Norway*

Complete contact information is available at: https://pubs.acs.org/10.1021/acs.energyfuels.5c00021

Notes

The authors declare no competing financial interest.

ACKNOWLEDGMENTS

B.H. acknowledges the Director CSIR-CIMFR for giving necessary permission to publish the work. B.H. also acknowledges the Science and Engineering Research Board, Department of Science and Technology, Government of India for the SERB International Research Experience award for the year 2023-2024 (Award Number: SIR/2022/001610).

REFERENCES

(1) Moore, T. A. Coalbed methane: a review. *Int. J. Coal Geol.* **2012**, *101*, 36–81.

(2) Pan, Z.; Wood, D. A. Coalbed Methane (CBM) Exploration, Reservoir Characterisation, Production, and Modelling: A Collection of Published Research (2009–2015). *J. Nat. Gas Sci. Eng.* **2015**, *26*, 1472–1484.

(3) Shi, J. Q.; Durucan, S. A Model for Changes in Coalbed Permeability during Primary and Enhanced Methane Recovery. *SPE Reservoir Eval. Eng.* **2005**, *8* (4), 291−299.

(4) Yao, Y.; Liu, D.; Tang, D.; Tang, S.; Huang, W. Fractal Characterization of Adsorption-Pores of Coals from North China: An Investigation on CH4 Adsorption Capacity of Coals. *Int. J. Coal Geol.* **2008**, *73* (1), 27−42.

(5) Li, Y.; Tang, D.; Elsworth, D.; Xu, H. Characterization of Coalbed Methane Reservoirs at Multiple Length Scales: A Cross-Section from Southeastern Ordos Basin, China. *Energy Fuels* **2014**, *28* (9), 5587−5595.

(6) Zhao, J.; Xu, H.; Tang, D.; Mathews, J. P.; Li, S.; Tao, S. A Comparative Evaluation of Coal Specific Surface Area by CO_2 and N_2 Adsorption and Its Influence on CH_4 Adsorption Capacity at Different Pore Sizes. *Fuel* **2016**, *183*, 420−431.

(7) Chandra, D.; Vishal, V. A Comparative Analysis of Pore Attributes of Sub-Bituminous Gondwana Coal from the Damodar and Wardha Valleys: Implication for Enhanced Coalbed Methane Recovery. *Energy Fuels* **2022**, *36* (12), 6187−6197.

(8) Safaei-Farouji, M.; Sethi, C.; Hazra, B.; Gao, Y.; Fattahi, E.; Vishal, V.; Pandey, J. K.; Ostadhassan, M. CO_2 Storage Potential of Coaly Shales of the Barakar Formation in the Rajmahal Basin, India. *Energy Fuels* **2024**, *38* (15), 14173−14187.

(9) Sing, K. S. Reporting Physisorption Data for Gas/Solid Systems with Special Reference to the Determination of Surface Area and Porosity (Recommendations 1984). *Pure Appl. Chem.* **1985**, *57* (4), 603−619.

(10) Gamson, P. D.; Beamish, B. B.; Johnson, D. P. Coal Microstructure and Micropermeability and Their Effects on Natural Gas Recovery. *Fuel* **1993**, *72* (1), 87−99.

(11) Everett, D. H. IUPAC Manual of Symbols and Terminology. *Pure Appl. Chem.* **1972**, *31*, 578.

(12) Perera, M. S. A.; Ranjith, P. G.; Choi, S. K.; Airey, D.; Weniger, P. Estimation of Gas Adsorption Capacity in Coal: A Review and an Analytical Study. *Int. J. Coal Prep. Util.* **2012**, *32* (1), 25−55.

(13) Liu, D.; Qiu, F.; Liu, N.; Cai, Y.; Guo, Y.; Zhao, B.; Qiu, Y. Pore Structure Characterization and Its Significance for Gas Adsorption in Coals: A Comprehensive Review. *Unconventional Resour.* **2022**, *2*, 139−157.

(14) Hazra, B.; Chandra, D.; Vishal, V. *Unconventional Hydrocarbon Reservoirs: Coal and Shale*; Springer: Cham, Springer Nature Switzerland, 2024.

(15) Li, X.; Kang, Y.; Haghighi, M. Investigation of Pore Size Distributions of Coals with Different Structures by Nuclear Magnetic Resonance (NMR) and Mercury Intrusion Porosimetry (MIP). *Measurement* **2018**, *116*, 122−128.

(16) Chandra, D.; Vishal, V. A Comparison of Nano-Scale Pore Attributes of Barakar Formation Gas Shales from Raniganj and Wardha Basin, India Using Low-Pressure Sorption and FEG-SEM Analysis. *J. Nat. Gas Sci. Eng.* **2020**, *81*, No. 103453.

(17) Hazra, B.; Vishal, V.; Singh, D. P. Applicability of Low-Pressure CO_2 and N_2 Adsorption in Determining Pore Attributes of Organic-Rich Shales and Coals. *Energy Fuels* **2021**, *35* (1), 456−464.

(18) Bhapkar, P. V.; Pradhan, S. P.; Chandra, D.; Hazra, B.; Vishal, V. Systematic pore characterization of sub-bituminous coal from Sohagpur coalfield, central India using gas adsorption coupled with X-ray scattering and high-resolution imaging. *Energy Fuels* **2023**, *37* (13), 9297−9308.

(19) Mahamud, M. M.; Novo, M. F. The use of fractal analysis in the textural characterization of coals. *Fuel* **2008**, *87* (2), 222−231.

(20) Liu, X.; Nie, B. Fractal characteristics of coal samples utilizing image analysis and gas adsorption. *Fuel* **2016**, *182*, 314−322.

(21) Hazra, B.; Wood, D. A.; Vishal, V.; Varma, A. K.; Sakha, D.; Singh, A. K. Porosity controls and fractal disposition of organic-rich Permian shales using low-pressure adsorption techniques. *Fuel* **2018**, *220*, 837−848.

(22) Li, Z.; Liu, D.; Cai, Y.; Wang, Y.; Teng, J. Adsorption pore structure and its fractal characteristics of coals by N_2 adsorption/desorption and FESEM image analyses. *Fuel* **2019**, *257*, No. 116031.

(23) Wang, Z.; Cheng, Y.; Qi, Y.; Wang, R.; Wang, L.; Jiang, J. Experimental study of pore structure and fractal characteristics of pulverized intact coal and tectonic coal by low temperature nitrogen adsorption. *Powder Technol.* **2019**, *350*, 15−25.

(24) Wood, D. A. Deriving Coal fractal dimensions from low-pressure nitrogen adsorption isotherms applying an integrated method. *Appl. Geochem.* **2021**, *131*, No. 105042.

(25) Yang, R.; He, S.; Yi, J.; Hu, Q. Nano-scale pore structure and fractal dimension of organic-rich Wufeng-Longmaxi shale from Jiaoshiba area, Sichuan Basin: Investigations using FE-SEM, gas adsorption and helium pycnometry. *Mar. Pet. Geol.* **2016**, *70*, 27−45.

(26) Hazra, B.; Chandra, D.; Vishal, V.; Ostadhassan, M.; Sethi, C.; Saikia, B. K.; Pandey, J. K.; Varma, A. K. Experimental study on pore structure evolution of thermally treated shales: implications for CO_2 storage in underground thermally treated shale horizons. *Int. J. Coal Sci. Technol.* **2024**, *11* (1), 61−78.

(27) Mastalerz, M.; Drobniak, A.; Rupp, J. Meso-and micropore characteristics of coal lithotypes: implications for CO_2 adsorption. *Energy Fuels* **2008**, *22* (6), 4049−4061.

(28) Hazra, B.; Wood, D. A.; Singh, P. K.; Singh, A. K.; Kumar, O. P.; Raghuvanshi, G.; Singh, D. P.; Chakraborty, P.; Rao, P. S.; Mahanta, K.; Sahu, G. Source-rock properties and pore structural framework of the gas-prone Lower Permian shales in the Jharia basin, India. *Arabian J. Geosci.* **2020**, *13*, 507.

(29) Nie, B.; Zhao, D.; He, X.; Kong, F.; Zhang, H.; Liu, X.; Deng, B.; Lun, J. Insights into the nanoscale microstructure diversity of different rank coals. *Energy Fuels* **2022**, *36* (18), 10899−10909.

(30) Fu, H.; Yan, D.; Yao, C.; Su, X.; Wang, X.; Wang, H.; Li, Y. Pore structure and multi-scale fractal characteristics of adsorbed pores in marine shale: a case study of the Lower Silurian Longmaxi shale in the Sichuan Basin. *China. J. Earth Sci.* **2022**, *33* (5), 1278−1290.

(31) Shi, X.; Liang, Z.; Yang, Y.; Li, Y.; Jiang, Z.; Li, Y.; Li, R.; Deng, F. Tectonic control on shale pore structure and gas content from the Longmaxi Formation Shale in Southern Sichuan Basin, China: Insights from fractal analysis and low-pressure gas adsorption. *Processes* **2023**, *11* (10), 2873.

(32) Chakraborty, P.; Hazra, B.; Sarkar, P.; Singh, A. K.; Singh, P. K.; Kumar, S. Thermal behavior of some Indian coals: inferences from simultaneous thermogravimetry−calorimetry and rock−eval. *Nat. Resour. Res.* **2021**, *30* (3), 2161−2177.

(33) Hazra, B.; Singh, D. P.; Crosdale, P. J.; Singh, V.; Singh, P. K.; Gangopadhyay, M.; Chakraborty, P. Critical insights from Rock-Eval analysis of vitrains. *Int. J. Coal Geol.* **2021**, *238*, No. 103717.

(34) ISO 7404−2. *Methods for the Petrographic Analysis of Coals—Part 2: Methods of Preparing Coal Samples*; International Organization for Standardization: Geneva, Switzerland, 2009.

(35) ISO 7404−5. *Methods for the Petrographic Analysis of Coals—Part 5: Method of Determining Microscopically the Reflectance of vitrinite*; International Organization for Standardization: Geneva, Switzerland, 2009.

(36) ISO 7404−3. *Methods for the Petrographic Analysis of Coals—Part 3: Method of Determining Maceral Group Composition*; International Organization for Standardization: Geneva, Switzerland, 2009.

(37) Lafargue, E.; Marquis, F.; Pillot, D. Rock-Eval 6 applications in hydrocarbon exploration, production, and soil contamination studies. *Rev. Inst. Fr. Pétrole* **1998**, *53* (4), 421−437.

(38) Behar, F.; Beaumont, V.; Penteado, H. L. D. B. Rock-Eval 6 technology: performances and developments. *Oil Gas Sci. Technol.* **2001**, *56* (2), 111−134.

(39) Hazra, B.; Dutta, S.; Kumar, S. TOC Calculation of Organic Matter Rich Sediments Using Rock-Eval Pyrolysis: Critical Consideration and Insights. *Int. J. Coal Geol.* **2017**, *169*, 106−115.

(40) Hazra, B.; Wood, D. A.; Mani, D.; Singh, P. K.; Singh, A. K.*Evaluation of Shale Source Rocks and Reservoirs*; Springer International Publishing: Berlin/Heidelberg, Germany, 2019; Vol. *142*.

(41) Carvajal-Ortiz, H.; Gentzis, T. Critical Considerations When Assessing Hydrocarbon Plays Using Rock-Eval Pyrolysis and Organic Petrology Data: Data Quality Revisited. *Int. J. Coal Geol.* **2015**, *152*, 113−122.

https://doi.org/10.1021/acs.energyfuels.5c00021
Energy Fuels 2025, 39, 5818−5831

(42) Hazra, B.; Wood, D. A.; Kumar, S.; Saha, S.; Dutta, S.; Kumari, P.; Singh, A. K. Fractal Disposition, Porosity Characterization and Relationships to Thermal Maturity for the Lower Permian Raniganj Basin Shales, India. *J. Nat. Gas Sci. Eng.* **2018**, *59*, 452−465.

(43) Singh, D. P.; Chandra, D.; Vishal, V.; Hazra, B.; Sarkar, P. Impact of Degassing Time and Temperature on the Estimation of Pore Attributes in Shale. *Energy Fuels* **2021**, *35* (19), 15628−15641.

(44) Yang, F.; Ning, Z.; Liu, H. Fractal Characteristics of Shales from a Shale Gas Reservoir in the Sichuan Basin, China. *Fuel* **2014**, *115*, 378−384.

(45) Li, A.; Ding, W.; He, J.; Dai, P.; Yin, S.; Xie, F. Investigation of Pore Structure and Fractal Characteristics of Organic-Rich Shale Reservoirs: A Case Study of Lower Cambrian Qiongzhusi Formation in Malong Block of Eastern Yunnan Province, South China. *Mar. Pet. Geol.* **2016**, *70*, 46−57.

(46) Ross, D. J. K.; Bustin, R. M. The Importance of Shale Composition and Pore Structure upon Gas Storage Potential of Shale Gas Reservoirs. *Mar. Pet. Geol.* **2009**, *26* (6), 916−927.

(47) Kuila, U.; Prasad, M. Specific Surface Area and Pore-Size Distribution in Clays and Shales. *Geophys. Prospect.* **2013**, *61* (2), 341−362.

(48) Dąbrowski, A. Adsorption—From Theory to Practice. *Adv. Colloid Interface Sci.* **2001**, *93* (1−3), 135−224.

(49) Günay, A.; Arslankaya, E.; Tosun, İ. Lead Removal from Aqueous Solution by Natural and Pretreated Clinoptilolite: Adsorption Equilibrium and Kinetics. *J. Hazard. Mater.* **2007**, *146* (1−2), 362−371.

(50) Thommes, M.; Kaneko, K.; Neimark, A. V.; Olivier, J. P.; Rodriguez-Reinoso, F.; Rouquerol, J.; Sing, K. S. Physisorption of Gases, with Special Reference to the Evaluation of Surface Area and Pore Size Distribution (IUPAC Technical Report). *Pure Appl. Chem.* **2015**, *87* (9−10), 1051−1069.

(51) Goodarzi, F.; Gentzis, T.; Grasby, S. E.; Dewing, K. Influence of igneous intrusions on thermal maturity and optical texture: Comparison between a bituminous marl and a coal seam of the same maturity. *Int. J. Coal Geol.* **2018**, *198*, 183−197.

(52) Hazra, B.; Singh, D. P.; Chakraborty, P.; Singh, P. K.; Sahu, S. G.; Adak, A. K. Using Rock-Eval S4Tpeak as Thermal Maturity Proxy for Shales. *Mar. Pet. Geol.* **2021**, *127*, No. 104977.

(53) Rouquerol, J.; Rouquerol, F.; Llewellyn, P.; Maurin, G.; Sing, K.*Adsorption by Powders and Porous Solids: Principles, Methodology, and Applications*; Academic Press: San Diego, CA, 2013.

(54) Gan, H.; Nandi, S. P.; Walker, P. L., Jr. Nature of the Porosity in American Coals. *Fuel* **1972**, *51* (4), 272−277.

(55) Parkash, S.; Chakrabartty, S. K. Microporosity in Alberta Plains Coals. *Int. J. Coal Geol.* **1986**, *6* (1), 55−70.

(56) Mahajan, O. P. Physical Characterization of Coal. *Powder Technol.* **1984**, *40* (1−3), 1−15.

(57) Mahajan, O. P. CO_2 Surface Area of Coals: The 25-Year Paradox. *Carbon* **1991**, *29* (6), 735−742.

(58) Mastalerz, M.; Drobniak, A.; Schimmelmann, A. Changes in Optical Properties, Chemistry, and Micropore and Mesopore Characteristics of Bituminous Coal at the Contact with Dikes in the Illinois Basin. *Int. J. Coal Geol.* **2009**, *77* (3−4), 310−319.

(59) Okolo, G. N.; Everson, R. C.; Neomagus, H. W.; Roberts, M. J.; Sakurovs, R. Comparing the Porosity and Surface Areas of Coal as Measured by Gas Adsorption, Mercury Intrusion, and SAXS Techniques. *Fuel* **2015**, *141*, 293−304.

(60) Anderson, R. B.; Hofer, L. J.; Bayer, J. Surface Area of Coal. *Fuel* **1962**, *41*, 559−564.

(61) Walker, P. L., Jr.; Verma, S. K.; Rivera-Utrilla, J.; Khan, M. R. A Direct Measurement of Expansion in Coals and Macerals Induced by Carbon Dioxide and Methanol. *Fuel* **1988**, *67* (5), 719−726.

(62) Lamond, T. G. Ph.D. Thesis, University of Durham: England, **1962**.

(63) Thomas, J. Jr.; Damberger, H. H. *Internal Surface Area, Moisture Content, and Porosity of Illinois Coals: Variations with Coal Rank*; Illinois State Geological Survey: Circular No. **1976**, *493*, 1-21.

(64) Mahajan, O. P.; Walker, P. L., Jr. Reactivity of Heat-Treated Coals. In *Analytical Methods for Coal and Coal Products*; Academic Press: New York, 1978; pp 465−494.

(65) Mandelbrot, B. B.; Wheeler, J. A. The Fractal Geometry of Nature. *Am. J. Phys.* **1983**, *51* (3), 286−287.

(66) Gregg, S. J.; Sing, K. S. W *Adsorption, Surface Area and Porosity*, 2nd ed.; Academic Press: London, 1982; 303 pp.

(67) Liu, S.; Xue, H.; Zhao, M. Pore Structure and Fractal Characteristics of Coal Measure Shale in the Wuxiang Block in the Qinshui Basin. *Processes* **2023**, *11*, 3362.

(68) Pfeifer, P.; Avnir, D. Chemistry in Noninteger Dimensions between Two and Three. I. Fractal Theory of Heterogeneous Surfaces. *J. Chem. Phys.* **1983**, *79* (7), 3558−3565.